Shahrood University of Technology

Journal of Mining and Environment (JME)

Journal homepage: www.jme.shahroodut.ac.ir

Iranian Society of Mining Engineering (IRSME)

Optimization of Delay Times for Reducing Blast-induced Ground Vibration in the Golgohar Mine Using the Signature Hole Analysis

Moein Bahadori[1*], Mohammad Amiri Hosseini[2] and Iman Atighi[3]

1. Faculty of Engineering, University of Gonabad, Gonabad, Iran
2. Head of Mining and Geology Research, Golghar Sirjan Mine Research and Technology Unit, Kerman, Iran
3. Department of Industrial engineering, Islamic Azad University, Kish, Iran

Article Info

Received 9 December 2024
Received in Revised form 18 March 2025
Accepted 6 April 2025
Published online 6 April 2025

DOI: 10.22044/jme.2025.15442.2960

Keywords

Blasting operations
Ground vibration
Optimum delay time
Superimpose waves
Signature Hole Analysis

Abstract

As open-pit mining advances, the decreasing separation between blast blocks and surface structures necessitates rigorous control of induced ground vibrations to mitigate structural risks. This study performed 13 single-hole blasting operations at the Golgohar Sirjan Iron Mine processing plant to evaluate vibration control strategies for protecting the onsite processing plant. A Blastmate III seismograph was employed to record 54 three-component data sets, including waveform data, maximum amplitude, and dominant frequencies. By superimposing waves, optimal delay times (ODT) for the blast holes were determined and the corresponding effects on wave frequencies were analyzed. An experimental blasting pattern was designed based on the derived ODT values, and the impact on ground vibration was examined. The results indicated a 10% reduction in vibration levels with the proposed delay times. Furthermore, considering the minimum distance of 111 meters from the processing plant to the final pit and adhering to the DIN safety standard, it is recommended that blast holes with a maximum diameter of 165mm be used to ensure a safety factor of 15%. For distances exceeding 187 meters, blast holes with a 250mm diameter are recommended to maintain production efficiency and a safety factor of 50%.

1. Introduction

Despite technological advancements, drilling and blasting remain essential in mining and construction projects [1]. An explosion is a rapid physicochemical phenomenon releasing energy as light, sound waves, and shock waves, accompanied by high-pressure and high-temperature gaseous products [2]. In blasting operations, only 20-30% of the released energy is harnessed for rock fragmentation and pile , while the remainder manifests as undesirable effects such as ground and air vibrations, fly-rock, and back-break [3, 4]. The outcomes of blasting operations are governed by controllable parameters (burden, spacing, hole diameter, charge type, and delay times) and uncontrollable parameters (rock mass properties, proximity to surface structures, and groundwater conditions). To optimize the results, the design engineer must judiciously configure the controllable parameters while accounting for accounting for the inherent variability of uncontrollable factors [5, 6]. Ground vibration poses a significant concern due to its potential to damage adjacent structures. Peak Particle Velocity (PPV) is widely employed to predict ground vibrations. Although various empirical and numerical methods have been developed to estimate PPV, most primarily rely on two factors: the maximum charge weight per delay and the distance between the blast block and the monitoring point. Nonetheless, additional factors, including geological and geotechnical conditions, blast geometry, explosive properties, blasting direction, detonation delays, and stemming, also affect PPV [7]. Moreover, it is crucial to consider vibration frequencies in conjunction with PPV, as certain frequency levels corresponding to specific

Corresponding author: moein.bahadori@gmail.com (A. Bahadori)

PPV values may increase the risk to nearby structures [8].

Delay times, aside from affecting PPV, can significantly influence other outcomes of rock blasting, such as the size distribution of rock fragments, air blast, fly rock, muck-pile shape and movement, as well as back-break (or side-break) [9, 10]. A common method to reduce vibrations is to use delay times greater than 8 ms between charge detonations. Assuming that vibrations from each detonation act independently, this method can prevent constructive interference and higher ground vibration levels. However, interference and superposition of seismic waves at varying distances may alter vibration patterns due to the differential attenuation rates across wave frequencies during propagation, warranting further investigation on the effects of wave interference on ground vibration [2].

As mines extend to greater depths, blasting blocks are positioned closer to surface structures, necessitating enhanced measures to mitigate the destructive effects of blasting operations. To predict and control blasting outcomes, researchers have employed a combination of field studies [11-17], laboratory experiments [18-21], and numerical modeling [22-26]. Collectively, these methods provide valuable insights into the management of blast-induced effects.

Kamali and Ataei (2010) pioneered a comparative analysis of statistical, empirical, and artificial neural network (ANN) models for PPV prediction in the Karoun III dam project, demonstrating ANN's superiority with high correlation coefficients and minimal error [27]. In a follow-up study, the same authors (2010) validated empirical models as practical alternatives despite ANN's accuracy, emphasizing site-specific adaptability [28]. Advancements in computational techniques emerged with Ghasemi et al. (2012), who developed a Mamdani-based fuzzy logic model for Iran's Sarcheshmeh copper mine, outperforming conventional regression and empirical methods [29]. Similarly, Mohamadnejad et al. (2012) applied support vector machines (SVM) and general regression neural networks (GRNN) to the Masjed-Soleiman dam, revealing SVM's higher precision (R^2 = 0.946) and computational efficiency [30]. Ataei and Kamali (2012) further hybridized methods, integrating adaptive neuro-fuzzy inference systems (ANFIS) with empirical models to predict PPV in the Karoun III project, balancing accuracy and practicality [31]. Ataei (2013) underscored the limitations of universal PPV formulas, advocating for region-specific models tailored to geological and technical variables, as demonstrated in Karoun III's empirical correlations [32]. Bakhshandeh Amnieh and Bahadori (2014) utilized artificial neural networks (ANN) with backpropagation to predict ground vibrations from blasting at Gotvand Olya Dam, achieving high accuracy with a mean square error of 1.95 and a correlation coefficient of 0.995. The study determined a maximum permissible explosive charge of 47.00 kg per delay for safe blasting operations, ensuring compliance with the allowable vibration limit of 120 mm/sec for heavy concrete structures [33]. Mansouri and Ebrahimi Farsangi (2015) introduced linear superposition modeling in Sarcheshmeh mine, synthesizing seismograms to optimize inter-row delays (>40 ms) and reduce vibrations [34]. Ataei and Sereshki (2017) expanded this to limestone mines, combining genetic algorithms with regression to refine site-specific PPV predictors for Iran's Shahrood Cement Company [35]. Mohammadi et al. (2020) integrated imperialist competitive and k-means algorithms with TOPSIS to rank blasting patterns in Sungun copper mine, identifying Pattern 27 (burden: 3 m, spacing: 4 m) as optimal for minimizing vibrations [36]. Srivastava et al. (2021) validated machine learning's edge, with random forest (R^2 = 0.81) and SVM outperforming linear regression in PPV prediction [37]. Dao et al. (2021) addressed Vietnam's compensation disputes by proposing a 24/7 seismic monitoring system aligned with Circular 32/2019, emphasizing real-time data integrity over unreliable single-blast simulations [38]. Bahadori et al. (2024) investigated the mitigation of blast-induced ground vibrations in Gol-Gohar mine, Sirjan, where vibrations from surface expansion triggered power outages in the processing plant. Using UDEC software, the study validated field blasting data and determined that trenches exceeding 2m in length and placed over 3m from structures could reflect 60% of blast waves, significantly reducing energy transfer without requiring significant trench width [39].

The Signature Hole Analysis (SHA) technique has emerged as a prominent approach for evaluating blast performance [40-45]. Traditional methods for predicting blast-induced ground vibration often neglected the effects of delay times, leading to results that vary across different mines and blasting patterns. The SHA technique was introduced and developed to overcome this limitation. In 2020, Agrawal and Mishra pioneered an approach that derived a simplified sinusoidal equation from signature hole data, streamlining and

accelerating the simulation of blast wave propagation. Although based on the assumption of linear superposition of waveforms, their method achieved an approximately 15% improvement in prediction accuracy [40]. Subsequent research in 2020 applied this technique to large-scale bench blasts in dragline mining. By incorporating various delay sequences and assuming a uniform distribution of explosive charges, simulations demonstrated that fine-tuning the delay sequence could reduce PPV by up to 48.26% while enhancing prediction precision [42].

Further advancements occurred in 2021 with the advent of electronic detonators, which enabled precise control over blast timing and facilitated the deliberate creation of destructive interference among blast waves. This refined approach not only reduced PPV in most cases but also increased vibration frequencies, thereby diverting energy away from hazardous ranges [43]. Concurrently, Sharma et. al. (2021) investigated the effects of inter-row delays using a single-hole model representative of multi-hole blasting. Their findings indicated that a 92-millisecond delay significantly decreased both the vibrations and the occurrence of backbreak [44].

Table 1 provides a concise summary of these studies, detailing their methodologies, computational logic, limitations, simplifications, and key results.

Table 1. Comparative Analysis of Signature Hole Analysis Techniques for Blast-Induced Ground Vibration Prediction, Highlighting Methodologies, Computational Logic, Limitations, Simplifications, and Key Results.

Year & Authors	Methodology	Computational Logic	Weaknesses & Limitations	Simplifications	Key Results
2020 – Agrawal and Mishra	Derived a simplified sinusoidal equation from signature hole data to simulate blast waves.	Assumed a linear superposition of waveforms using a simple sinusoidal model.	Does not capture the nonlinear complexities and real behavior of blast waves.	Assumed linear behavior and utilized a simplified sinusoidal model.	Improved prediction accuracy by approximately 15%.
2020 – Singh, Agrawal and Mishra	Applied the technique to large-scale bench blasts in dragline mining by employing various delay sequences.	Used delay sequences and assumed a homogeneous distribution of explosive charges to model PPV.	Traditional empirical methods may lead to errors in predicting complex blast scenarios.	Assumed uniform distribution of charges and used fixed delay sequences.	Reduced PPV by up to 48.26% while enhancing prediction accuracy (with low RMSE).
2021 – Singh, Agrawal and Mishra	Employed electronic detonators for precise blast timing to deliberately create destructive interference among blast waves.	Induced destructive interference among blast waves to simultaneously control PPV and vibration frequency.	Requires advanced equipment that may not be available in all field conditions.	Assumed high precision in blast timing and predicted outcomes of destructive interference.	Reduced PPV in most cases and increased vibration frequency, effectively shifting energy away from hazardous ranges.
2021 – Sharma et al.	Investigated the effect of inter-row delays using a single-hole model as a representative of multi-hole blasts.	Optimized inter-row delays to reduce both vibrations and the occurrence of backbreak.	The single-hole model may not fully capture the complexities of multi-hole blasts; fixed delays have inherent limitations.	Employed a single-hole model and assumed a fixed delay (e.g., 92 ms).	A 92-ms delay significantly decreased vibrations and backbreak occurrences.

The SHA technique evaluates blast performance by analyzing the characteristics of individual blast holes. It assumes blast waves behave similarly across different blast holes within a typical production blasting block. This assumption permits the study of a representative blast hole to predict overall blasting performance. By recording ground vibrations from a single blast hole and integrating these data with different delay times, the optimal delay time for minimizing blast-induced vibrations can be determined.

Numerous researchers have employed the SHA method to mathematically model blast wave behavior. These models approximate the sinusoidal nature of ground vibrations generated by blasting and analyzing the interaction between the waves [40, 43, 46-49]. However, when SHA waves are expressed using trigonometric equations via Fourier expansion, the analysis can become considerably complex, often requiring up to 30 terms. This complexity can lead to extensive and, in some cases, impractical calculations.

Each blast-induced wave comprises three components —vertical, tangential, and radial— each with its own frequency and amplitude. Consequently, the resultant vibration wave from two blast holes cannot be calculated by simply adding the corresponding components of each

wave. Instead, the calculation requires the algebraic summation of the corresponding components from each wave source in the time domain, considering any time delays. For instance, the vertical component of the first wave must be summed with the vertical component of the second wave (accounting for their respective delays) to yield the resultant vertical component. This procedure is similarly applied to tangential and radial components. Ultimately, the overall resultant vibration is determined by the cube root of the sum of the squares of the three new components.

Conversely, reducing the number of trigonometric terms in the analysis can significantly affect the accuracy of the calculations. In this study, Microsoft Excel was used to discretely process the signals recorded by the seismograph, thereby enabling the evaluation of wave interference with millisecond-level precision.

At the Golgohar mine, vibration sensors have been installed to monitor the periodic failures in processing plant equipment. These sensors automatically cut off power when recorded vibrations exceed the permissible limit (typically 7 mm/s) to ensure equipment safety and prevent potential accidents. Although this safety measure is valuable, false shutdowns may disrupt mining operations, resulting in downtime, production losses, and financial implications. Moreover, as mines expand and surface pits approach processing plants, the likelihood of vibrations triggering these sensors increases, necessitating taking appropriate measures to minimize potential damage or disruption.

In response to these challenges, the present study employs SHA technique to prevent operational shutdowns caused by blasting-induced vibrations. The research involves analyzing blast wave characteristics through 13 single-hole blasting experiments, determines optimal delay times (ODT) to minimize vibration amplitude while potentially increasing the dominant frequency, and proposes a mathematical relationship for the variation of ODT with distance. Additionally, a blasting pattern design is recommended for areas adjacent to the processing plant, considering the permissible vibration limits in the DIN standard. This proposed method aims to optimize blasting operations without interfering with current mining processes or increasing production costs, while ensuring vibrations remain within acceptable limits.

2. Methodology

2.1. Geological conditions, location, and access routes to the Golgohar Sirjan Iron mine

The Golgohar Sirjan mine is situated approximately 60 kilometers southwest of Sirjan, at geographical coordinates of approximately 55°20' E and 29°05' N. It is located at the center of an equilateral triangle defined by the cities of Shiraz, Hormozgan, and Kerman, each at an approximate distance of 300 kilometers. Access to mine is primarily by the Sirjan-Shiraz Road. A secondary road branches off after 45 kilometers from Sirjan and extends for approximately 8 kilometers to the site.

Geologically, the Golgohar mining region lies on the eastern edge of the Sanandaj-Sirjan zone and the western margin of the Khairabad Salt Dome depression. The area is characterized by some of the oldest metamorphic rocks of the Paleozoic metamorphic belt, which host significant mineral deposits. The principal rock formations in the mining area include magnetite, hematite, mica-schist, quartzite, amphibolite, conglomerate, and sedimentary formations. Based on exploration data, the ore deposit is described as a lens-like structure trending northwest-southeast, with a proven reserve of approximately 152 million metric tons. The mine's annual production capacity is estimated at 10 million metric tons of iron ore and 8 million metric tons of waste material. Figure 1 illustrates the geographical location and access routes to the Golgohar Sirjan iron ore mine.

2.2. Drilling and Blasting Operation in Golgohar Mine

Blast hole drilling operations at the Golgohar mine are executed using drilling machines manufactured by Ingrasolrand, AtlasCopco, and Titon. These machines are equipped with drill bits of various diameters, 76mm, 89mm, 165mm, 203mm, and 250mm. Depending on the rock type and the presence of discontinuities, the blast holes are arranged in multiple patterns, including 3m×4m, 5m×6m, 5.5m×6.5m, 5.5m×7m, and 9m×11m, with an overall drilling depth of 17.5m (including 2.5m sub-drilling). ANFO is employed as the primary explosive, while emulsion is used for charging water-filled blast holes. Given the mine's metallic nature and the potential risk of unintended explosions, non-electric blasting systems are adopted, and, whenever possible, Nonel detonators with delay times of 17ms, 25ms, 42ms, 50ms, and 65ms are utilized to enhance operational safety.

Figure 1. The geographical location and access routes to the Golgohar Sirjan mine

2.3. Seismic sensors of the processing plant

Considering the specific focus of this paper on the performance of the sensors installed in the blasting section of the Golgohar Sirjan processing plant, particularly in managing vibrations induced by blasting operations, the following details outline the location and specifications of the installed sensors. Within the processing plant, seven seismic sensors manufactured by Brüel & Kjær Vibro with a vibration threshold of 7mm/s are installed to continuously monitor the normal vibrations of the mechanical equipment. In the event of malfunctions or when vibrations exceed the permissible limit, these sensors are designed to automatically halt operations, thereby preventing progressive damage to the plant.

Moreover, as the mine deepens and surface expansion becomes necessary, the distance between the blasting blocks and surface structures has decreased. This reduction results in higher levels of blast-induced ground vibrations reaching the constructed area. In some cases, when the stimulus wave exceeds the threshold, the power supply to the circuit is interrupted, resulting in the operational shutdowns that incur additional costs for the mining facility.

Figure 2 illustrates the vibration monitoring sensors installed on the pelletizing plant of the Golgohar Sirjan mine, specifically showing their mounting on the ball mill and dust collector structure.

Based on the field information from experts in the processing and electrical domains, the current breaker sensor is primarily designed to monitor abnormal oscillations in the plant's mechanical components to prevent potential hazards. Under normal operating conditions, machinery elements such as shafts, bearings, and other components generate specific vibrations with defined amplitudes and frequencies. Consequently, any deviation from these standard vibration patterns can be detected and identified as a pulse or unusual vibration. Thus, these sensors are not chiefly installed for monitoring ground vibrations induced by blasting operations but rather designed to monitor the health status of the mechanical components integral to the milling process.

2.4. Signature Hole Tests

Since the drilling of a single blasthole and its explosion incur significant costs and time, and can interfere with regular mining operations, this study proposes an alternative method to record and analyze blast waves from a single blasthole. In this approach, the first blasthole in each circuit is detonated with an optimized delay relative to the remaining blastholes, thereby ensuring that the vibrations can be separated analyzed independently.

To determine the ODT, an initial delay of 500 ms was used. However, as illustrated in Figure 3a, this delay failed to achieve proper separation between the waves generated by the first blasthole and those from the other blastholes in the circuit. Consequently, a subsequent experiment considered a delay of 1000 ms between the explosion of the first blasthole and the others. As shown in Figure 3 b, this delay produced a proper separation of the

generated waves, and therefore this delay value was used in subsequent blast recordings.

To analyze the seismic waves from the explosion in 13 blasting blocks, the first blasthole, with a 1000-ms delay, was connected to the rest of the circuit. This configuration ensured that the recorded wave from the first blasthole (signature hole) is well separated from the waves produced by the remaining circuit (production holes). Figure 4 shows the selected locations of the blasting blocks used for recording the explosion vibrations within the mine pit, and Table 2 presents the information obtained from the 13 field experiments of signature blasthole.

Based on these data, and with a focus on the blasthole charge, a wave attenuation curve of the blasting signature holes was derived. As shown in Figure 5, two nonlinear models, a power and an exponential function, have been proposed to predict ground vibration (PPV) resulting from the single blast holes, yielding R^2 values of 0.49 and 0.84, respectively. Notably, the power function, which has been widely used in previous studies for predicting PPV, showed lower compliance with measured data compared to the exponential function. This discrepancy may be attributed to the lower absorption rate of the blast wave from a single blast hole compared to a real pattern (with numerous blast holes) that exhibits higher attenuation.

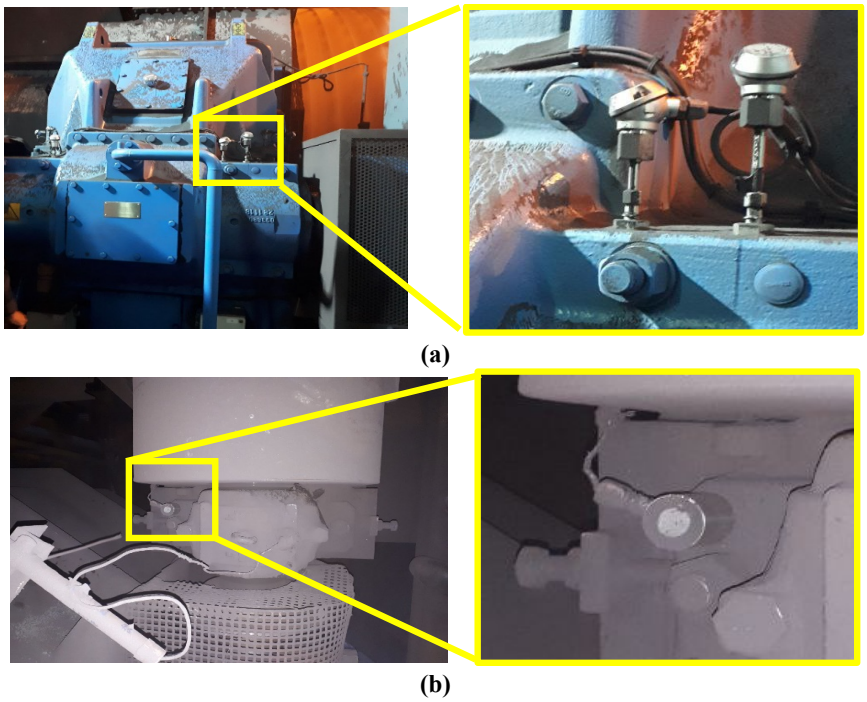

(a) **(b)**

Figure 2. Mechanical vibration monitoring sensors from Brüel & Kjær Vibro are installed placed on (a) ball mill electromotor and (b) fan

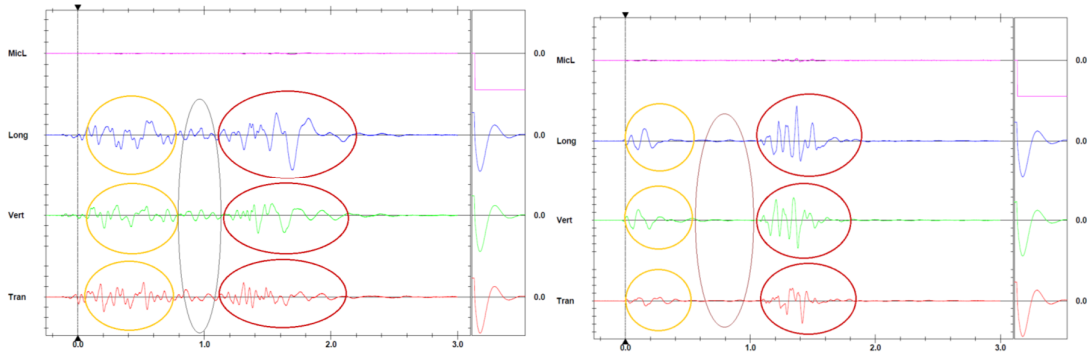

Figure 3. The effect of delay time on the wave separation between signature hole and production blasting with the delay time of 500 ms (left) and 1000 ms (right)

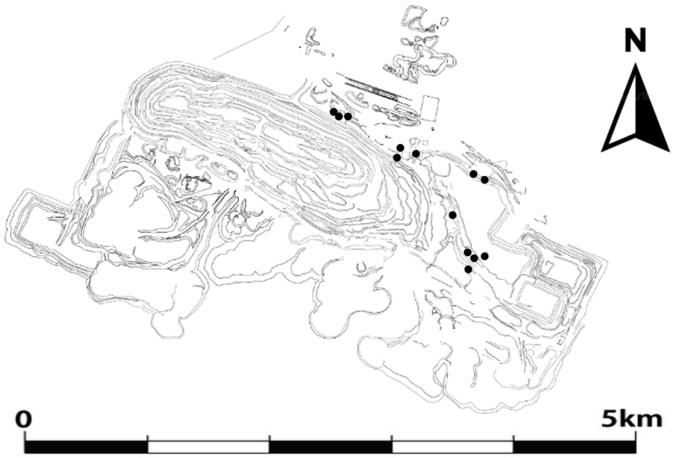

Figure 4. Locations of conducted SHA test in the Golgohar mine area

Table 2. Seismographic information and the method of depreciation from a signature blast hole in the conglomerate rock mass of Golgohar Sirjan mine

Row	Block Num.	Rock mass	Charge Weight (kg)	Distance to measuring location (m)	Scaled distance ($m/kg^{0.5}$)	PPV (mm/s)
1	6-881	Conglomerate	400	76.25	3.81	24.06
2	5-534	Conglomerate	400	100.12	5.01	47.64
3	5-532	Conglomerate	400	115.34	5.77	17.71
4	5-523	Conglomerate	400	98.11	4.91	42.45
5	8-983	Conglomerate	400	84.51	4.23	24.17
6	5-542	Conglomerate	400	96.8	4.84	24.77
7	7-994-1	Conglomerate	400	207.08	10.35	27.65
8	7-994-2	Conglomerate	400	102.30	5.12	47.30
9	4-181	Conglomerate	400	156.00	7.80	17.87
10	5-519	Conglomerate	400	81.00	4.05	7.52
11	7-1035-1	Conglomerate	400	40.67	2.03	203.34
12	7-1035-2	Conglomerate	400	30.68	1.53	295.59
13	8-1004-1	Conglomerate	400	20.12	1.01	225.76
14	8-1004-2	Conglomerate	400	10.29	0.51	259.15
15	11-840-1	Conglomerate	400	9.99	0.50	255.76
16	11-840-2	Conglomerate	400	20.98	1.05	278.26
17	9-963-1	Conglomerate	400	30.13	1.51	276.53
18	9-963-2	Conglomerate	400	39.58	1.98	250.64
$PPV = 218.54 \times SD^{-1.163}, R^2 = 0.4861$						(1)
$PPV = 263.05 \times \exp(-0.362 \times SD), R^2 = 0.8415$						(2)

Scaled distance (SD) is defined as the ratio of the distance from the wave source (i.e., the blasthole) to the measurement point, divided by the square root of the maximum charge weight per delay. The maximum charge weight per delay refers to the amount of explosive detonated within an 8 ms delay interval. Mathematically, this is expressed as d/W^0.5.

2.5. Frequency analysis of the signature blast holes

One detrimental effect of rock blasting-induced ground vibrations is related to the frequency of the generated waves. Increased vibration amplitude can cause damage when the frequency of the waves aligns the natural frequency range of nearby structures. To analyze the frequency characteristics of blast waves signature blastholes, the three components (longitudinal, transverse, and vertical components) recorded by the seismograph were evaluated using the fast Fourier transform analysis

method in Microsoft Excel. Figure 6 shows the dominant frequency curves for these tri-component signals from the signature blasthole of blasting block number 5-542.

Due to substantial variations in the dominant frequencies observed in this study, a Frequency-weighted averaging method was employed to derive an overall frequency value for the generated waves. The weighted average values of the signature hole frequencies are presented in Table 3. Notably, the duration of the waves from the blastholes relatively consistent, ranging from approximately 950 to 1060 ms, while the dominant frequencies from the blast waves varied between 10.9 to 39.54 hertz.

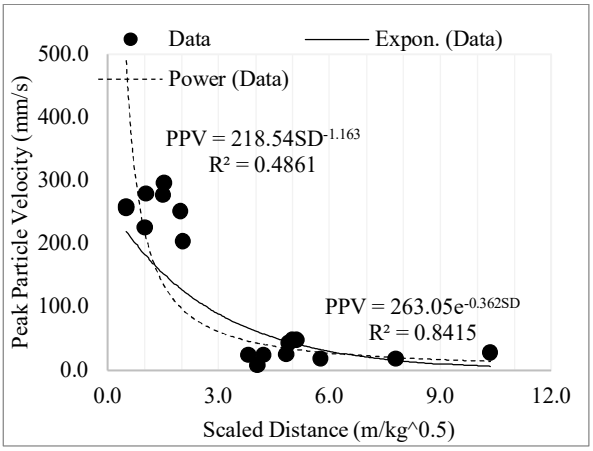

Figure 5. Mathematical equation for wave attenuation of the signature blast holes in Golgohar Mine

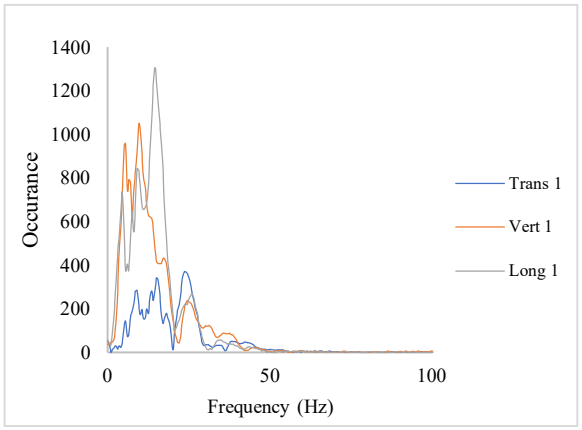

Figure 6. Fast Fourier transform and determination of dominant frequencies for tri-component of signature blast hole in pattern number 5-542

Table 3. Calculating the weighted average of the dominant frequency in the signature hole tests for tri-components and vector-sum

Row	Block Num.	Weighted average of dominant frequencies for signature blast experiments				
		Transverse (Hz)	Vertical (Hz)	Longitudinal (Hz)	Vector sum (Hz)	wave duration (ms)
1	6-881	18.27	18.29	13.91	13.29	1000
2	5-534	14.55	14.78	14.74	13.11	1000
3	5-532	13.86	16.37	14.40	12.49	950
4	5-523	12.49	14.05	17.91	14.23	980
5	8-983	14.05	17.79	13.60	15.30	955
6	5-542	21.10	14.72	14.60	15.24	995
7	7-994-1	20.46	16.57	11.58	16.03	950
8	7-994-2	14.71	15.89	11.31	16.56	965
9	4-181	13.27	12.07	10.90	10.59	985
10	5-519	13.88	11.50	11.56	9.89	1060
11	7-1035-1	19.28	20.91	27.19	18.37	970
12	7-1035-2	28.09	29.08	31.31	21.45	960
13	8-1004-1	24.23	38.49	22.53	20.83	965
14	8-1004-2	29.20	23.31	24.63	21.34	970
15	11-840-1	23.97	39.54	31.67	22.91	950
16	11-840-2	30.58	30.72	39.48	19.87	970
17	9-963-1	28.51	26.23	28.95	22.05	950
18	9-963-2	28.39	28.28	30.29	23.21	950

2.6. Determining the optimal delay time to minimize the energy of blast waves from two adjacent blast holes

In general, the propagation of waves in a medium is governed by both the characteristics of the wave source and the mechanical properties of the medium. Since geological and geotechnical variations within a blasting block are typically minimal and the blastholes exhibit consistent diameters and explosive material, it is expectable that the propagated waves from the individual blastholes will be similar. These assumptions constitute the fundamental basis for employing the blast analysis technique.

The main difference in the simplified model can be attributed to two factors: the time delay between the blastholes and the differences in distance between adjacent blastholes and the measurement station. Additionally, an important consideration is the difference in the propagation medium between the first blasthole and the subsequent ones. Specifically, the waves from the first blasthole travel through an elastic medium, while those from the subsequent blastholes propagate in a medium that may have experienced plastic or irreversible elastic deformations due to the previous blastholes.

In this study, owing to the complex nature of the deformation effects caused by blasthole detonations, it is assumed that the propagated waves occur in an elastic medium. Moreover, given the significant distance between the measurement station and the blastholes within a blasting block, the time differences in wave arrival at the measurement stations can be largely disregarded. Importantly, the delay time is not omitted; rather, it implies that the relative positions of the blast holes with respect to the measurement point are approximately the same.

For illustrative purposes, Figure 7 displays a sinusoidal wave with a frequency of 0.03 Hz. Assuming that this wave represents one of the three vibration components (radial, tangential, and vertical) generated by the blasting of a single hole in a blasting pattern, a superposition model was developed to examine how varying delay times can lead to either destructive or constructive interference. In this analysis, delay times between the two blast holes were varied from 10 and 50 ms in increments of 10 ms, and the corresponding impact on the amplitude of the resultant wave (the combined wave from both holes) was calculated.

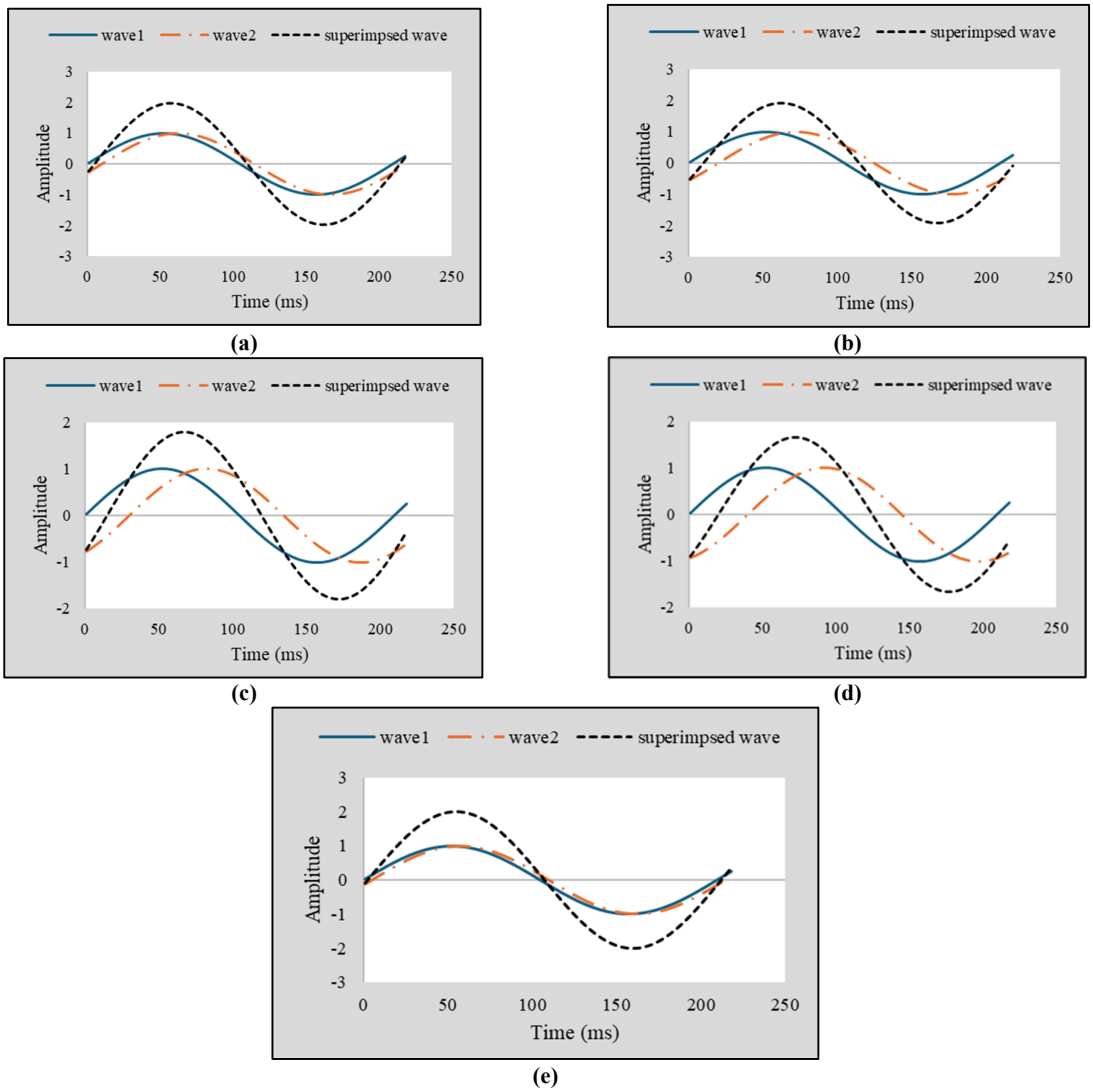

Figure 7. The effect of delay times on the vector sums for a simple sinusoidal wave with (a) 10 ms, (b) 20 ms, (c) 30 ms, (d) 40 ms, and (e) 50 ms.

Figure 8 illustrates the variations in amplitude resulting from the superposition of two similar sinusoidal waves as a function of time delay. The figure indicates that a time delay of 100 ms produces the most pronounced destructive interference between the two waves. Although this example represents a simplified case of one-dimensional wave propagation, it is important to note that the three components of ground vibration do not necessarily behave identically. Consequently, the optimal delay time that effectively attenuates one component (for example, 50 ms in Figure 8) may simultaneously amplify another. In essence, determining the delay time that minimizes the resultant amplitude of all three components from the two blast holes requires more complex calculations and a multidimensional approach.

When considering two wave components with different amplitudes and frequencies occurring simultaneously, the superposition of these components with varying delay times leads to more complex behavior in the resultant wave. Consequently, the optimum delay time for achieving the most destructive interference may differ from conditions observed under simpler scenarios. For example, Figure 9(a) and 9(b) illustrate a two-dimensional sinusoidal wave, characterized by amplitudes of 1 and 2 and frequencies of 0.03 and 0.08 Hz, respectively, along with its resultant wave. This wave is assumed to be generated by a single blast hole in two perpendicular directions. When this wave is superimposed with an identical wave but with varying delay times, different outcomes are observed. In this particular instance, the minimum destructive interference occurs at a delay time of 117 ms.

The phenomenon becomes even more complex when extending the analysis to three-dimensional waves with three distinct components. As depicted in Figure 9(c) and 9(d), the superposition of such a 3D wave with itself at various delay times yields significantly different results, with the most destructive interference occurring at a delay time of 46 ms.

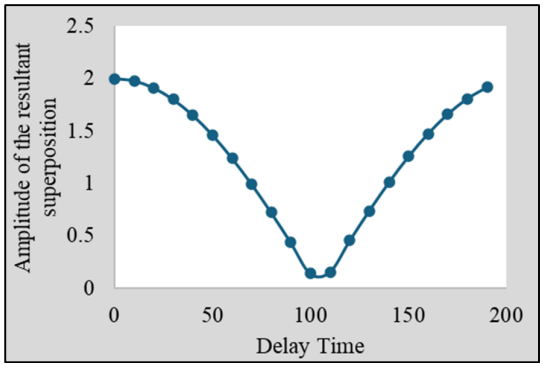

Figure 8. Variations of maximum vibration amplitude versus delay time

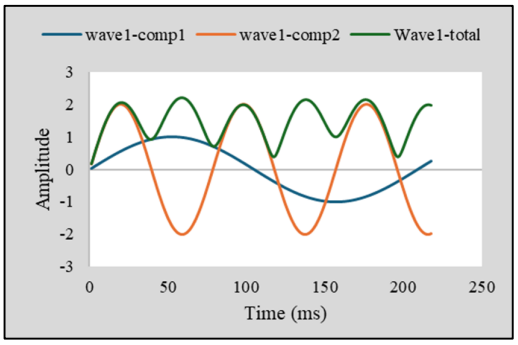

(a)

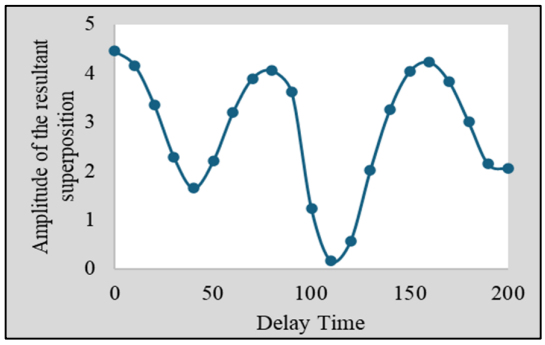

(b)

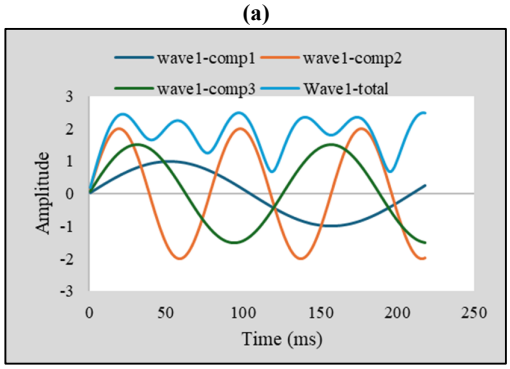

(c)

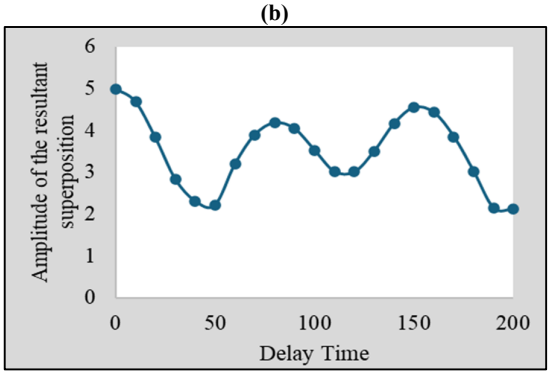

(d)

Figure 9. Superimposing 2D and 3D sinusoidal waves to achieve the most destructive results with changing in delay times.

In real blasting operations, it is generally assumed that the waves generated by each blast hole are identical, with differences in their arrival at the measurement station primarily due to the time delay introduced by time-delay relays. Based on this assumption, the interference of waves can vary significantly as the time delay between adjacent blast holes changes. At specific delay times, the maximum and minimum amplitudes of each vibration component may interfere destructively. However, the optimal delay time often varies across different vibration components. As a result, determining the delay time that minimizes the resultant vibration requires an optimization approach.

Since ground vibrations are recorded discretely by seismographs (e.g., the Blastmate III seismograph records data at a rate of 1024 Hz), the corresponding vibration values are also discrete. When two blast holes detonate with a specific time delay, their three perpendicular vibration components propagate in all directions. At any moment after the start of blasting, the value of each vibration component is equal to the vector sum of two contributions: (1) the vibration component of the first blast hole at that moment, and (2) the corresponding value from the same blast hole after the time delay between the two blast holes.

For example, suppose the longitudinal vibration of a single blast hole at the measurement station is 25 mm/s at 10 ms from the start of the blasting, and its vibration at 35 ms is -20 mm/s. If two blast holes detonate under identical conditions with a delay time of 25 ms, the longitudinal component at 35 ms would be expected to have a value of +5 mm/s. This principle applies to all three perpendicular vibration components. Consequently, a clear relationship can be established between time delay and the destructive interference of waves.

It is important to note that due to varying vibration frequencies in different directions, the interference patterns of the perpendicular components are not necessarily identical (see Table 3). For instance, while destructive interference might occur for longitudinal waves at a delay time of 25 ms (as in the example above), the interference in other directions may be constructive, amplifying the resultant vibrations. Therefore, a comprehensive analysis is necessary to determine the delay time that minimizes the vector sum of the vibration components. This is calculated using the following equation:

$$PV_S(t) = sqrt\left(PV_V^2(t) + PV_L^2(t) + PV_T^2(t)\right) \quad (3)$$

in which PV_S represents the magnitude of the resultant vibration component at time t after the start of the blasting, while PV_V, PV_L, and PV_T represent the ground vibration components in the vertical, longitudinal, and transverse directions, respectively. The value of each component for two-hole blasting that has occurred with the delay time interval of dt is calculated as follows:

$$\begin{aligned} PV_V(t) &= PV_V1(t) + PV_V2(t) \\ PV_L(t) &= PV_L1(t) + PV_L2(t) \\ PV_T(t) &= PV_T1(t) + PV_T2(t) \end{aligned} \quad (4)$$

Using index 1 to denote the first blast hole and index 2 to denote the second blast hole, and assuming the waves emitted by both the blast holes have the same pattern, we can infer that the value of each perpendicular vibration component from the second blast hole at time t is equal to its corresponding value in the first blast hole at time t+dt. Therefore, the vibration components of the second blast hole can be expressed as follows:

$$\begin{aligned} PV_V2(t) &= PV_V1(t+dt) \\ PV_L2(t) &= PV_L1(t+dt) \\ PV_T2(t) &= PV_T1(t+dt) \end{aligned} \quad (5)$$

Based on the information provided, equation (4) can be rewritten as follows:

$$\begin{aligned} PV_V(t) &= PV_V1(t) + PV_V1(t+dt) \\ PV_L(t) &= PV_L1(t) + PV_L1(t+dt) \\ PV_T(t) &= PV_T1(t) + PV_T1(t+dt) \end{aligned} \quad (6)$$

Given the discrete nature of the data, for each vibration component, the value PV2 = PV1(t+dt) is calculated in MS Excel using the VLOOKUP function. This value is then vectorially added to PV1(t), and the resulting sum is used to calculate the resultant vibration magnitude. Considering the impact of varying time delays on the resultant ground vibration by the two-hole blasting, identifying the delay time that minimizes the maximum vibrations is an optimization problem. This optimization was performed using the Solver tool in MS-Excel, and for each single-hole experiment, the optimal time value was obtained that minimizes the resultant ground vibrations.

For clarity, Figure 10 illustrates the variations in the sum of the resultant components with changes in the time delay. As observed, the maximum vibration levels vary with the time delay, and the resultant vibration from blasting is plotted as a function of the time delay. Based on

these observations, for block 5-542, located 105 meters away from the seismograph, a time delay of 49.5 ms minimizes the maximum blast-induced waves (20.85 mm/s), which is even lower than the vibration magnitude generated by a single blasthole (24.76 mm/s). Notably, within the time delay range between 28 ms and 52 ms, the resultant vibration from the two-hole blasting is consistently lower than that from single-hole blasting. This range is called the Appropriate Delay Time (ADT), with the optimized delay of 49.5 ms referred to as the Optimal Delay Time (ODT).

t is important to note that the minimization of the three perpendicular components does not occur simultaneously at a single time delay. Specifically, the minimum values are observed at 44 ms for the longitudinal component, 63 ms for the transverse component, and 55 ms for the vertical component.

This process was extended to three and four blast holes, and the impact of time delay on the resultant blast wave component was analyzed using the following equation (7). This equation demonstrates that although the magnitude of the resultant component increases with the number of blast holes, the obtained ODT value for minimizing vibrations remains valid even for more than two blast holes.

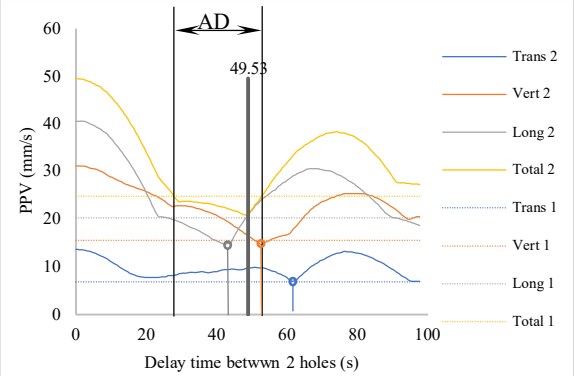

Figure 10. Influence of the delay times on PPV and tri-component of blasting two adjacent holes in block No. 5-542.

$$
\begin{aligned}
PV_{Vn}(t) &= PV_V 1(t) + PV_V 1(t+dt) + PV_V 1(t+2dt) + \ldots + PV_V 1(t+ndt) \\
PV_{Ln}(t) &= PV_L 1(t) + PV_L 1(t+dt) + PV_L 1(t+2dt) + \ldots + PV_L 1(t+ndt) \\
PV_{Tn}(t) &= PV_T 1(t) + PV_T 1(t+dt) + PV_T 1(t+2dt) + \ldots + PV_T 1(t+ndt)
\end{aligned} \tag{7}
$$

Furthermore, to examine the effect of the optimal time delay on the frequency of generated waves, the sum of the resultant vibration components for the two-hole blasting at ODT was compared with those from the single-hole setup. In this study, the weighted average of the dominant frequencies was used. This method calculates an average frequency in which each dominant frequency is weighted according to its corresponding amplitude or energy, thereby assigning greater importance to frequencies with higher amplitudes and providing a more accurate representation of the overall vibration behavior in the system. For example, for block 5-542, with ODT of 49.5 ms, the weighted average dominant frequencies for the longitudinal, transverse, and vertical components changed from 21.1 Hz, 14.72 Hz, and 14.6 Hz in the single-hole scenario to 22.57 Hz, 15.70 Hz, and 15.48 Hz in the two-hole configuration, respectively. All these frequencies are outside the hazardous range (i.e., the natural frequencies of surface structures, which typically range from 5 to 15 Hz). This analysis was repeated for all three vibration components.

According to the analyses, both the ODT and ADT values vary for different blast holes. Table 4 presents the calculated values for each blast hole. Figure 11 illustrates the change in the weighted average dominant frequencies for the single-hole and two-hole blasting using the optimal delay time for each pattern. In most cases, the selected time delay resulted in a modification of dominant frequencies: compared to the single hole, the lower frequencies generally increased while the higher frequencies decreased. This modification causes a broader distribution of blast-induced wave energy across the frequency spectrum. In some cases, this broader distribution prevents the accumulation of energy at hazardous frequencies, a benefit achieved by using the ODT. For example, in the vertical component, the weighted average predominant frequency is shifted out of the dangerous zone in pattern No. 5-542, and a similar shift is observed in the transverse component for patterns No. 5-534, 8-893, 7-994-2, and 5-519. Although some weighted average dominant frequencies remain within the hazardous range, the observed changes suggest that use of ODT (or at least ADT) can reduce the amplitude of vibrations and thereby help limit potential damages.

Table 4. Effects of ODT on weighted average of the dominant frequency of tri-component and vector sum of blasting two adjacent blast holes

Row	Block num.	ODT (ms)	ADT (ms)		Transverse (Hz)	Vertical (Hz)	Longitudinal (Hz)	Vector sum (Hz)
			from	to				
1	6-881	36.13	24.42	39.61	19.23	18.78	13.82	15.93
2	5-534	35.16	29.35	47.9	15.03	14.66	14.78	14.62
3	5-532	40.04	32.24	45.9	13.34	17.15	14.94	17.18
4	5-523	42.97	34.16	56.55	13.17	14.37	18.61	14.85
5	8-983	48.83	38.08	66.38	16.27	19.43	15.21	16.46
6	5-542	48.83	26.43	51.76	22.57	15.70	15.48	16.74
7	7-994-1	59.57	55.69	62.48	20.71	18.70	11.74	17.25
8	7-994-2	42.97	39.09	46.90	15.36	17.49	11.06	16.96
9	4-181	62.50	45.88	68.41	14.32	12.82	11.68	12.28
10	5-519	62.50	45.92	70.27	15.55	12.98	13.11	13.11
11	7-1035-1	43.95	36.13	62.53	19.79	21.09	28.58	15.78
12	7-1035-2	31.25	23.44	36.13	26.44	26.85	28.83	19.54
13	8-1004-1	25.39	22.16	35.14	21.43	40.76	18.79	18.89
14	8-1004-2	44.92	38.09	48.83	31.19	21.51	21.80	18.18
15	11-840-1	28.32	25.39	31.23	21.06	36.93	24.25	18.90
16	11-840-2	32.23	26.34	35.16	27.82	22.75	31.75	16.25
17	9-963-1	36.13	33.12	44.38	24.64	21.64	24.87	18.93
18	9-963-2	35.16	28.65	39.44	25.26	25.93	27.33	19.41

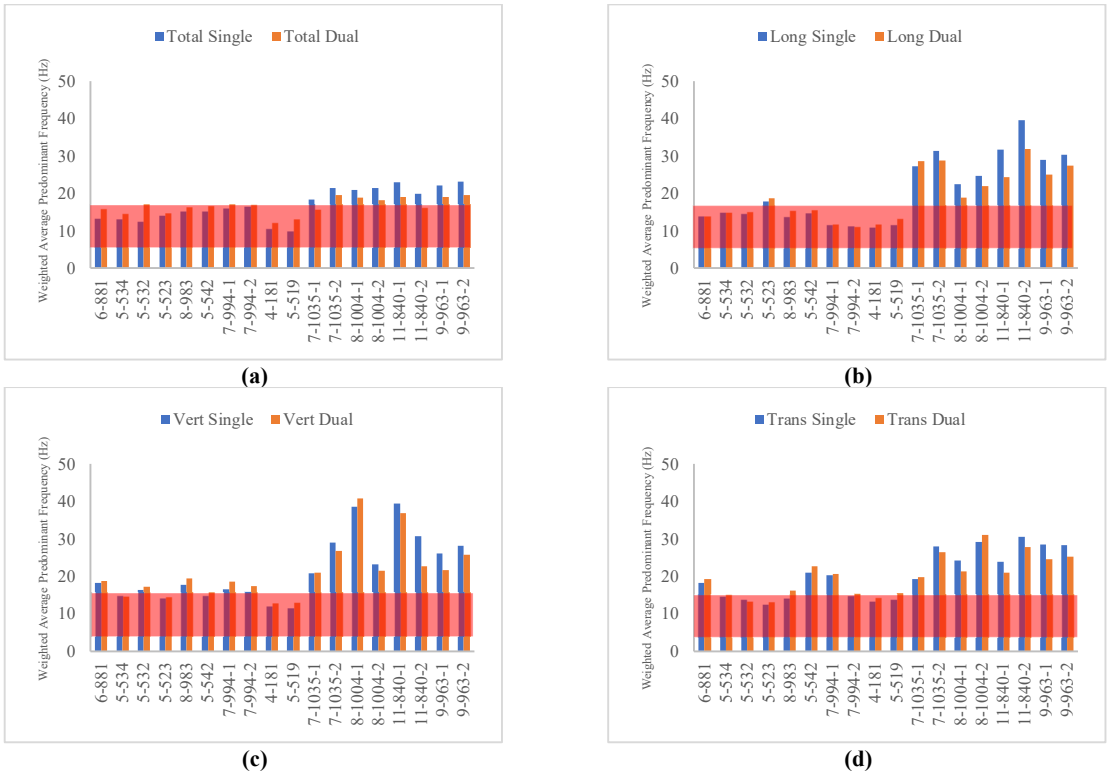

Figure 11. Changing the weighted average domain frequency from signature hole to superimposing two adjacent blast holes, natural frequencies of surface structures are highlighted in red color

The propagation of blast waves in geological materials is significantly influenced by the dispersive nature of the Earth's medium, meaning that the velocity of wave propagation depends on frequency. This dispersion can be characterized by examining both phase velocity and group velocity.

Phase velocity represents the speed at which individual wave crests or single-frequency components travel through the medium. In dispersive environments such as the Earth's crust, lower-frequency waves (longer wavelengths) typically propagate faster because they penetrate

deeper layers with lower impedance. Conversely, higher-frequency waves (shorter wavelengths) are more sensitive to surface properties and tend to travel more slowly.

Group velocity, on the other hand, refers to the speed at which the energy or information contained within a wave packet propagates. This parameter is particularly critical in blast wave analysis as it governs how the bulk energy from a blast spreads through the Earth's layers. High-frequency components generally have slower group velocities, leading to the temporal stretching of wave pulses, a phenomenon known as wave dispersion.

After any blasting operation, a broad spectrum of frequencies is generated. Low-frequency components, which can penetrate deeper, typically propagate faster, whereas high-frequency components are attenuated more rapidly and remain largely confined to near-surface layers, propagating at lower velocities. This frequency-dependent behavior results in temporal stretching of the wave pulse, primarily due to differences in group velocity and energy dissipation, as high-frequency waves lose energy more quickly through scattering and absorption.

Since the velocity of wave propagation depends on frequency, and considering that blast waves consist of various frequency components, it is expected that with an increase in the distance from the wave source, the vibrational energy of the waves will be distributed over a longer time range, leading to a separation of wave frequencies. Consequently, the optimal time delay for reducing vibrations is likely to be a function of distance. Figure 12 illustrates the relationship between the optimal time delays and the distance between the measurement station and the signature hole. Despite some statistical scattering, the data reveal an ascending trend: as the distance between the blasting block and the sensitive structure (or measurement point) increases, the optimal time delay required to reduce the range of vibrations also increases.

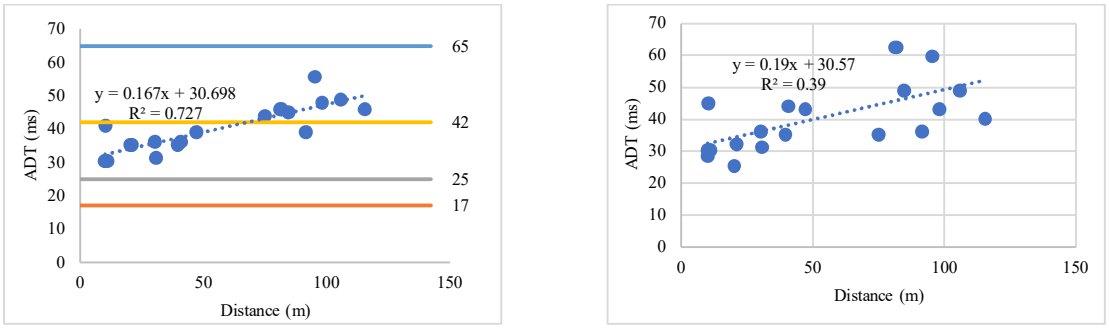

(a) **(b)**

Figure 12. Changes in the delay time to obtain the ground vibrations with increasing distance from the blast hole in Golghar mine

In the next step, to improve the fitted regression line and better understand the relationship between delay times and distance, we assume that the optimal time delay can vary within the ADT range. Notably, this range is still lower than the PPV of the two-hole blasting compared to that of the single-hole blasting. As shown in Figure 9, when the ADT is used as the allowable delay between the two holes, the coefficient of determination (R^2) increases from 0.39 to 0.73. Next, this refined curve is used as a criterion to determine the optimal time delay. This curve is then used as a criterion to determine the optimal delay between two blast holes; it provides in-row delay time for each distance from the blast block with the desired accuracy.

However, applying this refined curve requires access to electronic detonators, a system not currently available at the Golgohar mine. Therefore, alternative systems, such as the "Nonel" system, must be used. While the Nonel system offers a wide range of delay times, it does not cover all the desired values. In each case, the closest available delay time should be selected. Specifically, if the required ODT between two blast holes is less than the average value between two consecutive delays in the Nonel system, the closest available delay value should be chosen.

Furthermore, it is essential not to overlook the permissible vibration limits determined by relevant standards. If these limits are exceeded, additional measures should be taken to prevent damage to surface structures. These measures include reducing the hole diameter, using decoupling techniques, modifying the layout to ensure proper alignment of wave interference, employing presplit

blasting, or digging a trench along the wave propagation path.

2.7. Verification of the results using field experiment

To investigate the impact of delay times and layout on the quality of blast-induced seismic waves, a field test was conducted in the conglomerate rock mass of Golgohar mine. In this test, two rows of blast holes, each with a diameter of 10 inches and containing an average of 400 kilograms of explosive material (ANFO), were drilled and detonated. The weight of explosives in each hole was controlled by the ANFO-truck monitoring system, which has an approximate error of ±5%.

It is important to note that, as described in earlier tests aimed at improving wave separation and isolating the waves emitted by the signature hole, the first hole in each pattern was always detonated with a 1000 millisecond delay compared to the other holes. However, this delay was not applied in the current field test. As a result, it is not possible to achieve the actual waves by combining and interfering with the waves. Nonetheless, by comparing the expected vibration levels (calculated using empirical equations) with the measured values from the seismograph, the effectiveness of the proposed method can be assessed.

Figure 13 (a) illustrates the sequence of hole ignition in the blast pattern, while Figure 13 (b) and 10c depict, respectively, the position of the seismograph relative to the blast block and the pile movement of the fragmented rocks after the operation. As shown in Figure 13 (c), delay times of 25 and 65 ms were utilized in this experiment.

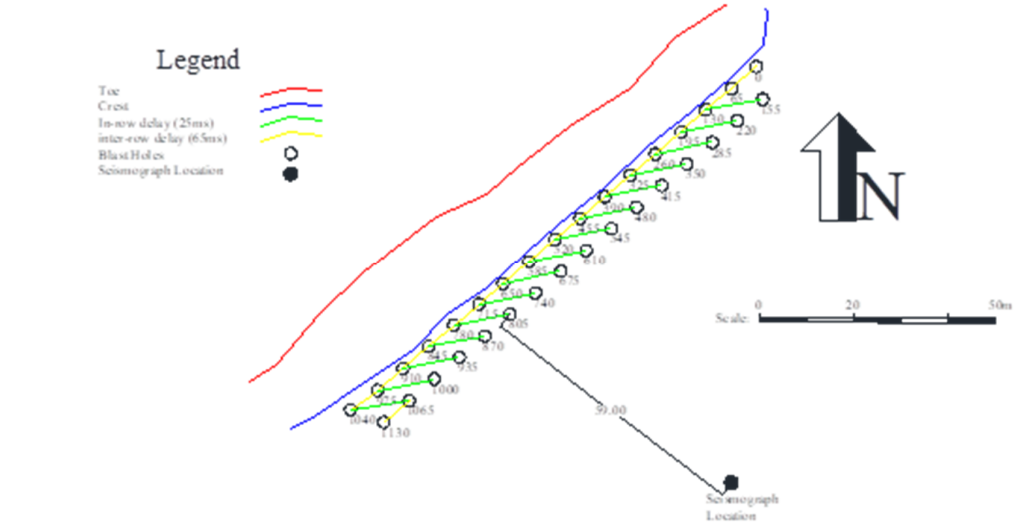

(a)

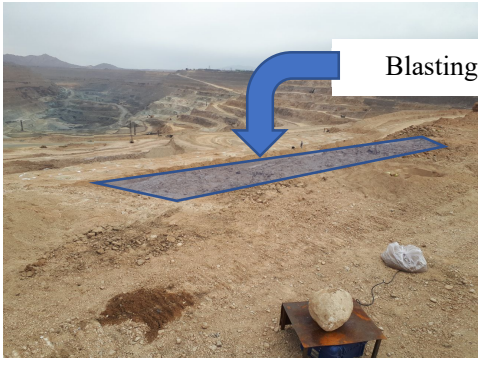

(b)

(c)

Figure 12. The field experiment of rock blasting

According to the derived power-law relationship in Figure 5, the predicted ground vibration for this block, based on a minimum distance of 59.09 meters between the blast hole and the sensor location, is estimated at 90.27 mm/s when 400 kilograms of explosive material are used

per blast hole. However, the seismograph recorded a value of 81.61 mm/s, reflecting an approximate 10% reduction in ground vibration due to the application of the proposed delay times. It is important to note that, when modifying the layout using this method, one must also consider potential changes in the behavior of fragmented mass movement and the final position of the muck-pile, as these factors can significantly impact the loading and hauling efficiency of the mine.

3. Discussion

Based on what was presented in this research, two principal mitigation strategies were proposed to reduce ground vibration induced by blasting operations: layout modification and blast hole diameter reduction. Additionally, by considering the conservative DIN standard, which sets the maximum allowable particle velocity at the processing plant site to be 18 mm/s, the results obtained from the previous analyses for different distances can be used to establish a limit on the charge weight per delay. In other words, this limit informs the selection of blast hole diameter and, ultimately, the design of the blast pattern based on the proposed blast hole diameter.

To address this issue, it is imperative to determine the final pit position next to the processing plant before performing any calculations. This step allows for the definition of specific zones within the mine by determining the distance between the structure and potential blast block locations. As shown in Figure 11, the closest distance between the processing plant and the final pit is approximately 111 meters. Therefore, given this distance and the permissible vibration limit of 18 mm/s, the maximum charge weight per delay in the mine's standard blasting operations needs to be determined.

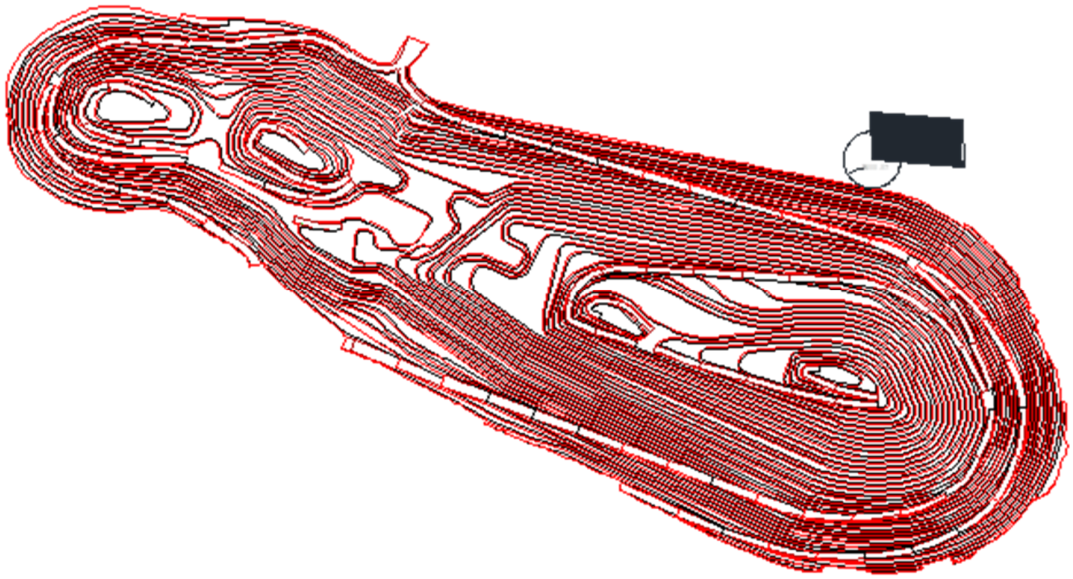

Figure 14. The location of the factory is next to the final pit of Golgohar mine, with the closest distance of 111 m.

Based on the closest distance of 111 meters between the processing plant and the final pit of mine, the maximum allowable charge weight per delay is calculated to be 225 kilograms, according to the accuracy of the mathematical equation (2). Consequently, it is recommended to use 165mm blast holes for this closest distance while adhering to the layout modifications proposed in this research.

Considering the total blast hole length of the 17.5 meters and a stemming length of 5.5 meters (resulting in a charge length of 12 meters), the approximate consumption of explosive material per blast hole is around 173 kilograms, given that the longitudinal density of charge in a blast hole is approximately 17 kg/m). By applying the proposed wave attenuation equation, the resulting ground vibration from this blast is to be about 15.67mm/s, thereby providing a 15% safety factor.

In extensive mining operations such as at Golgohar, the use of larger diameter blast holes is generally preferred. For distances greater than 162 meters between the processing plant and the blast block, the use of 250mm blast holes appears feasible. Moreover, by targeting a safety factor of 1.5, the effective use of 250mm blast holes can be extended to distances greater than 187 meters.

It is worth noting that the vibration levels recorded at the processing plant, as measured by the on-site sensors, still exceed the defined permissible value of 7 mm/s. The long-term effect of these vibrations on the performance and operation of the production line's mechanical components is another important aspect that needs to be investigated. This requires analyzing the history of mechanical vibrations recorded by the sensor(s) over a carefully chosen time interval. This time interval should capture the vibration variations of the production line before the two recent overhaul stages. Such an analysis would help evaluate changes in vibration quality before each overhaul stage and during the normal operations, assessing the impact of excitatory vibrations (such as blasting) on it. Although these vibrations occur almost daily, and have occasionally caused power outages at the concentration plant, field research and expert assessments indicate that these events do not significantly impact the regular maintenance of production equipment..

In summary, the proposed method facilitates both the prediction and optimization of blasting results. Traditional mathematical equations neglect the effect of delay times, which can lead to uncertain and scattered results. In contrast, superimposing real data without simplification provides more precise outcomes, characterized by lower scatter and reduced error.

Despite its widespread application in predicting blast-induced ground vibrations, the SHA technique has several limitations that can affect its accuracy. Notably, it relies on simplified assumptions that do not fully capture the nonlinear interactions between blast holes, geological fractures, and geomechanical conditions. Its heavy dependence on empirical data and the omission of key parameters, such as rock type and porosity, can further compromise prediction accuracy. Additionally, it typically considers one-dimensional wave propagation, whereas in reality, seismic waves propagate in a three-dimensional environment influenced by geological and topographical factors. The linear modeling of blast delays also falls short, as unexpected wave superposition may alter vibration patterns. Other limitations include the exclusion of environmental factors like groundwater conditions and natural fractures, as well as reduced accuracy in predicting vibrations at greater distances.

Many of these limitations are common to traditional blast prediction methods. Nevertheless, the SHA technique remains a more accurate and efficient approach. Ultimately, integrating its results with advanced numerical models, such as artificial neural networks, holds significant promise for effectively mitigating these limitations and enhancing overall predictive performance.

4. Conclusions

Controlling blast-induced ground vibrations is a critical challenge in large-scale open-pit mining, particularly when the distance between blast blocks and adjacent structures is reduced. At the Golgohar mine, vibration monitoring systems automatically halt processing operations upon detecting abnormal vibrations. Although this measure prevents equipment damage, it can lead to costly false alarms resulting from blast-induced vibrations. In response to this issue, the present study analyzed 13 single-hole blasts, recording 54 vibration components, and developed a regression model ($R^2 = 0.84$) based on the SHA to assess wave attenuation. Unlike similar studies that rely on simplified assumptions, this research incorporated real ground vibration data without approximation, ensuring higher accuracy in predicting wave propagation and attenuation. The findings demonstrated that optimal delay times (ODT) significantly reduced peak particle velocity through destructive wave interference, sometimes shifting wave frequencies out of the hazardous 5–15 Hz range. Moreover, a direct relationship between ODT and blast distance was identified, with an accuracy of 0.73 achieved within the allowable adjustment delay time (ADT). Considering the constraints of the Nonel system, optimized ODTs were proposed for various distances, resulting in a 10% reduction in PPV during field tests.

Based on the DIN standard, the maximum charge weight per delay at a distance of 111 meters from the processing plant was determined to be 320 kg, which corresponds to a longitudinal blasting density of 27 kg/m. Overall, this study highlights the effectiveness of precise timing in mitigating blast vibrations and underscores the benefits of a data-driven approach that minimizes simplifying assumptions. Future research should explore integrating SHA with advanced numerical models and machine learning techniques to further enhance predictive accuracy and optimize delay time selection.

Conflict of interest

The authors declare that they have no conflict of interest.

References

[1]. Rodríguez, R., García de Marina, L., Bascompta, M., & Lombardía, C., (2021), Determination of the ground vibration attenuation law from a single blast: A particular case of trench blasting, *Journal of Rock Mechanics and Geotechnical Engineering, 13*(5), 1182-1192

[2]. Jimeno, C. L., Jimeno, E. L., Carcedo, F. J. A., & de Ramiro, Y. V., (1995), *Drilling and Blasting of Rocks* (USA: CRS Press).

[3].Hustrulid, W., (1999), *Blasting Principles for Open Pit Mining*. Rotterdam, Netherlands: AA Balkema.

[4]. Garai, D., Agrawal, H., & Mishra, A. K., (2023), Impact of orientation of blast initiation on ground vibrations, *Journal of Rock Mechanics and Geotechnical Engineering, 15*(1), 255-261

[5]. Taiwo, B. O., Yewuhalashet, F., Ogunyemi, O. B., Babatuyi, V. A., Okobe, E. I., & Orhu, E. A., (2023), Quarry slope stability assessment methods with blast induced effect monitoring in Akoko Edo, Nigeria, *Geotechnical and Geological Engineering, 41*(4), 2553-2571

[6]. Zhang, X., Yan, P., Lu, W., Cheng, Y., Sun, C., Zhu, J., Guo, W., & Cheng, X., (2023), Frequency spectrum characteristics of blast-induced vibration with electronic detonators in ground blasting, *Journal of Building Engineering, 74*(1), 106892

[7]. Soltani-Mohammadi, S., Bakhshandeh Amnieh, H., & Bahadori, M., (2011), Predicting ground vibration caused by blasting operations in Sarcheshmeh copper mine considering the charge type by Adaptive Neuro-Fuzzy Inference System (ANFIS), *Archives of Mining Sciences, 56*(4), 701-710.

[8]. Siskind, D. E., Strachura, V. J., Stagg, M. S., & Kopp, J. W., (1980), *Structure Response And Damage Produced By Airblast From Surface Mining*. US Department of the Interior, Bureau of Mines.

[9]. Soltanalinejad, S. & Moomivand, H., (2024), Development of a novel empirical approach to control overbreak, surface quality, and slope angle of benches following blasting, *Canadian Geotechnical Journal, 62*(1), 1-22

[10]. Moomivand, H., Soltanalinejad, S., & Karwansara, A. M., (2025), Assessment of the optimized stemming length considering rock fragmentation and escape of explosive gases using actual large-scale results, *Results in Engineering, 25*(1), 103575

[11]. Bohloli, B., (1997), Effects of the geological parameters on rock blasting using the Hopkinson split bar, *International Journal of Rock Mechanics and Mining Sciences, 34*(3-4), 32-e1

[12]. Esen, S., Onederra, I., & Bilgin, H., (2003), Modelling the size of the crushed zone around a blasthole, *Int. J. Rock Mech. Min. Sci., 40*(4), 485-495

[13]. Iverson, S. R., Hustrulid, W. A., Johnson, J. C., & Akbarzadeh, Y., (Year), The extent of blast damage from a fully coupled explosive charge, in *Proceedings of the 9th International Symposium on Rock Fragmentation by Blasting, Fragblast 9*, Granada, Spain, J. Sanchidrián, Ed., 2010: CRC Press: Taylor and Francis Group. 459-468.

[14]. Bahadori, M., (2022), Designing the surface and underground blasting operations to avoid damage to concrete structures in Gotvand Olya dam using genetic algorithm, *Geotechnical and Geological Engineering, 40*(12), 5685-5699

[15]. Kahraman, E. & Kilic, A. M., (2023), Determination of the effective blasting region by using fragmentation analysis: A field study, *Iranian Journal of Science, 47*(3), 791-799

[16]. Ding, X., Bahadori, M., Hasanipanah, M., & Abdullah, R. A., (2023), Predicting the rock fragmentation in surface mines using optimized radial basis function and cascaded forward neural network models, *Geomechanics and Engineering, 33*(6), 567-581

[17]. Yu, C., Shi, X., Gao, Q., Zhang, X., & Wang, F., (2023), Research on the evolution law of the seismic wave field based on the explosive source parameters, *Frontiers in Earth Science, 11*(1), 1-12

[18]. Xiao, C., Yang, R., Zhao, Z., You, S., He, S., & Zhang, Y., (2023), Blasting damage control of slit charge structure, *Mechanics of Advanced Materials and Structures, 31*(25), 6848–6862

[19]. Meng, Q., Wang, H., Wang, P., Qu, Y., Zhang, Y., Zhang, H., & Zhang, W., (2023), An optimized destress blasting design for hard roof during early mining stage: A case study, *Geotechnical and Geological Engineering, 41*(1), 4775–4793

[20]. Zairov, S. S., Urinov, S. R., Tukhtashev, A. B., & Borovkov, Y. A., (2020), Laboratory study of parameters of contour blasting in the formation of slopes of the sides of the career, *Technical science and innovation, 2020*(3), 81-90

[21]. Bohloli, B., Gustafson, G., & Ronge, B., (2001), A laboratory study on reducing the quantity of rock fines at failure: application to rock blasting and crushing, *Bulletin of Engineering Geology and the Environment, 60*(4), 271-276

[22]. Uyar, G. G. & Aksoy, C. O., (2019), Comparative review and interpretation of the conventional and new methods in blast vibration analyses, *Geomechanics and Engineering, 18*(5), 545-554

[23]. Li, Z., Hu, Y., Wang, G., Zhou, M., Hu, W., Zhang, X., & Gao, W., (2023), Study on cyclic blasting failure characteristics and cumulative damage evolution law of tunnel rock mass under initial in-situ stress, *Engineering Failure Analysis, 150*(1), 107310

[24]. Gao, F., Tang, L., Yang, C., Yang, P., Xiong, X., & Wang, W., (2023), Blasting-induced rock damage control in a soft broken roadway excavation using an air deck at the blasthole bottom, *Bulletin of Engineering Geology and the Environment, 82*(3), 97

[25]. Li, X., Liu, K., Qiu, T., Sha, Y., Yang, J., & Song, R., (2023), Numerical study on fracture control blasting using air–water coupling, *Geomechanics and Geophysics for Geo-Energy and Geo-Resources, 9*(1), 29

[26]. Ye, Z., Chen, M., Yi, C., Lu, W., & Yan, P., (2023), Quantitative study of the action on rock mass failure under the shock wave and gas pressure in bench blasting, *International Journal of Geomechanics, 23*(9), 04023135

[27]. Kamali, M. & Ataei, M., (2010), Prediction of blast induced vibrations in the structures of Karoun III power plant and dam, *Journal of Vibration and Control, 17*(4), 541-548

[28]. Kamali, M. & Ataei, M., (2010), Prediction of blast induced ground vibrations in Karoun III power plant and dam:

a neural network, *Journal of the South African institute of mining and metallurgy (SAIMM), 110*(1), 1-10.

[29]. Ghasemi, E., Ataei, M., & Hashemolhosseini, H., (2012), Development of a fuzzy model for predicting ground vibration caused by rock blasting in surface mining, *Journal of Vibration and Control, 19*(5), 755-770

[30]. Mohamadnejad, M., Gholami, R., & Ataei, M., (2012), Comparison of intelligence science techniques and empirical methods for prediction of blasting vibrations, *Tunnelling and Underground Space Technology, 28*(2), 238-244

[31]. Ataei, M. & Kamali, M., (2012), Prediction of blast-induced vibration by adaptive neuro-fuzzy inference system in Karoun 3 power plant and dam, *Journal of Vibration and Control, 19*(12), 1906-1914

[32]. Ataei, M., (2010), Evaluation of blast induced ground vibrations from underground excavation at Karoun 3 area, *Mining Technology, 119*(1), 7-13

[33]. Bakhshandeh Amnieh, H. & Bahadori, M., (2014), Safe vibrations of spilling basin explosions at "Gotvand Olya Dam" using artificial neural network, *Archives of Mining Sciences, 59*(4), 1087-1096

[34]. Mansouri, H. & Ebrahimi Farsangi, M. A., (2015), Blast vibration modeling using linear superposition method, *Journal of Mining and Environment, 6*(2), 125-140

[35]. Ataei, M. & Sereshki, F., (2017), Improved prediction of blast-induced vibrations in limestone mines using Genetic Algorithm, *Journal of Mining and Environment, 8*(2), 291-304

[36]. Mohammadi, D., Mikaeil, R., & Abdollahei Sharif, J., (2020), Investigating and Ranking Blasting Patterns to Reduce Ground Vibration using Soft Computing Approaches and MCDM Technique, *Journal of Mining and Environment, 11*(3), 881-897

[37]. Srivastava, A., Choudhary, B. S., & Sharma, M., (2021), A Comparative Study of Machine Learning Methods for Prediction of Blast-Induced Ground Vibration, *Journal of Mining and Environment, 12*(3), 667-677

[38]. Dao, H., Pham, T. L., & Hung, N. P., (2021), Study on an Online Vibration Measurement System for Seismic Waves Caused by Blasting for Mining in Vietnam, *Journal of Mining and Environment, 12*(2), 313-325

[39]. Bahadori, M., Bemani, M., Atighi, I., & Amiri Hosseini, M., (2024), Optimization of Trench Dimensions to Reduce Blast-Induced Ground Vibration in Gol-Gohar Sirjan Mine Using Numerical Modeling, *Journal of Analytical and Numerical Methods in Mining Engineering (ANM), 14*(39), 47-58

[40]. Agrawal, H. & Mishra, A. K., (2020), An innovative technique of simplified signature hole analysis for prediction of blast-induced ground vibration of multi-hole/production blast: an empirical analysis, *Natural Hazards, 100*(1), 111-132

[41]. Dumakor-Dupey, N. K., Arya, S., & Jha, A., (2021), Advances in blast-induced impact prediction—a review of machine learning applications, *Minerals, 11*(6), 601

[42]. Singh, C. P., Agrawal, H., & Mishra, A. K., (2021), Frequency channeling: a concept to increase the frequency and control the PPV of blast-induced ground vibration waves in multi-hole blast in a surface mine, *Bulletin of Engineering Geology and the Environment, 80*(10), 8009-8019

[43]. Singh, C. P., Agrawal, H., & Mishra, A. K., (2020), A study on influence of blast-induced ground vibration in dragline bench blasting using signature hole analysis, *Arabian Journal of Geosciences, 13*(13), 522

[44]. Sharma, M., Choudhary, B. S., Kumar, H., & Agrawal, H., (2021), Optimization of delay sequencing in multi-row blast using single hole blast concepts, *Journal of The Institution of Engineers (India): Series D, 102*(2), 453-460

[45]. Yang, R., Pratt, L., & Zhao, G., (2023), A case study on trim blast fragmentation optimization using the MBF model and the MSW blast vibration model at an open pit mine in canada, *Rock Mechanics and Rock Engineering, 56*(5), 3641-3658,

[46]. Ghosh, A. & Daemen, J. J. K., (1983), A simple new blast vibration predictor (based on wave propagation laws)," presented at the The 24th U.S. Symposium on Rock Mechanics (USRMS), Texas 1983.

[47]. Sambuelli, L., (2009), Theoretical derivation of a peak particle velocity–distance law for the prediction of vibrations from blasting, *Rock Mechanics and Rock Engineering, 42*(3), 547-556,

[48]. Chen, S.-h., Hu, S.-w., Zhang, Z.-h., & Wu, J., (2017), Propagation characteristics of vibration waves induced in surrounding rock by tunneling blasting, *Journal of Mountain Science, 14*(12), 2620-2630, doi:

[49]. Aldas, G. G. U. & Ecevitoglu, B., (2008), Waveform analysis in mitigation of blast-induced vibrations, *Journal of Applied Geophysics, 66*(1), 25-30,

انجمن مهندسی معدن ایران
نشریه مهندسی معدن و محیط زیست
نشانی نشریه: www.jme.shahroodut.ac.ir
دانشگاه صنعتی شاهرود

بهینه‌سازی زمان‌های تأخیر به منظور کاهش لرزش زمین ناشی از انفجار در معدن گلگهر سیرجان با استفاده از تکنیک چال شاخص

معین بهادری[1*]، محمد امیری حسینی[2] و ایمان عتیقی[3]

۱. گروه مهندسی معدن و عمران، دانشکده فنی و مهندسی، مجتمع آموزش عالی گناباد، خراسان رضوی، ایران
۲. رئیس تحقیقات معدن و زمین شناسی، واحد تحقیقات و فناوری معدن گلگهر سیرجان، کرمان، ایران
۳. دانشکده مهندسی صنایع، دانشگاه آزاد اسلامی، کیش، ایران

اطلاعات مقاله

تاریخ ارسال: ۲۰۲۴/۱۰/۰۹
تاریخ داوری: ۲۰۲۵/۰۳/۱۸
تاریخ پذیرش: ۲۰۲۵/۰۴/۰۶

DOI: 10.22044/jme.2025.15442.2960

کلمات کلیدی

عملیات انفجار
لرزش زمین
زمان تأخیر بهینه
امواج روی هم قرار گرفته
تحلیل حفره‌های دارای مشخصه

چکیده

استخراج مس پورفیری مقادیر قابل‌توجهی باطله تولید می‌کند که به دلیل توانایی در تولید اسید و آزادسازی عناصر بالقوه سمی، مخاطرات جدی زیست‌محیطی و بهداشتی برای انسان به همراه دارد. در این مطالعه، ارزیابی یکپارچه‌ای از ریسک‌های زیست‌محیطی و سلامت انسانی ناشی از باطله‌های معدن مس پورفیری سونگون در شمال‌غرب ایران ارائه شده است. بدین منظور، رویکردی جامع و میان‌رشته‌ای به کار گرفته شد که شامل ترکیب آنالیزهای فیزیکوشیمیایی، کانی‌شناسی و ژئوشیمیایی با روش‌های آماری بود. گونه‌بندی شیمیایی عناصر با استفاده از روش اصلاح‌شده پیشنهادی دفتر مرجع جامعه اروپا انجام شد؛ روشی که در مطالعات متعدد برای ارزیابی تفکیک ژئوشیمیایی و تحرک‌پذیری عناصر به کار رفته است. هدف اصلی این پژوهش، گذار از تحلیل صرف غلظت کل عناصر به سوی ارزیابی دقیق‌تر ریسک مبتنی بر زیست‌دسترس‌پذیری، با بهره‌گیری از چارچوب سازمان حفاظت محیط‌زیست ایالات متحده برای کودکان و بزرگسالان بود. بررسی‌های کانی‌شناسی نشان داد که باطله‌ها دارای پتانسیل خالص تولید اسید هستند، به‌گونه‌ای که مقدار پیریت (حدود ۴ درصد) معمولاً بیش از کانی خنثی‌کننده اصلی، یعنی کلسیت (حدود ۲ درصد)، است. نتایج آنالیزهای ژئوشیمیایی بیانگر غنی‌شدگی قابل‌توجه مس و مولیبدن و همچنین غنی‌شدگی متوسط آرسنیک و کبالت در باطله‌ها بود. در میان عناصر مورد بررسی، بیشترین ضرایب تحرک به ترتیب متعلق به مس (۸۱٫۴۹٪)، سرب (۷۶٫۷۱٪)، روی (۷۱٫۶۵٪) و مولیبدن (۵۹٫۲۷٪) بود. شاخص خطر غیرسرطان‌زایی برای کودکان برابر با ۲٫۰۴ به‌دست آمد که از حد ایمنی فراتر است و در این میان، وانادیم زیست‌دسترس‌پذیر به‌عنوان عامل اصلی ریسک شناسایی شد. این یافته‌ها نشان می‌دهد که اتکای صرف بر غلظت کل عناصر بالقوه سمی می‌تواند گمراه‌کننده باشد و بر ضرورت انجام ارزیابی‌های مبتنی بر گونه‌پذیری شیمیایی برای توصیف دقیق رفتار زیست‌محیطی و مخاطرات سلامت ناشی از باطله‌های معدنی تأکید می‌کند.

نویسنده مسئول مکاتبات: *moein.bahadori@gmail.com* (م. بهادری)